Comparison of Simplistic System-Level RIS Models and Diffraction-Theory Solutions

Le Hao*, Francisco S. Cuesta†, and Sergei A. Tretyakov†
*Institute of Telecommunications, TU Wien (Technical University Wien), Vienna, Austria
†Department of Electronics and Nanoengineering, Aalto University, Espoo, Finland
le.hao@tuwien.ac.at

***Abstract*—We discuss and compare two recently published path-loss models for reconfigurable intelligent surfaces (RIS) derived from the electromagnetic and communication theory points of view. The electromagnetic model considers the RIS as a whole, taking into account field interactions of all metasurface elements, whereas the communication model is based on an assumption that each array element is an independent relay. The estimations given by the two models are rather different but, surprisingly, we find that the simplistic model gives the same result as the electromagnetic calculation for perfectly functioning anomalous reflectors if one replaces the effective areas of the unit cells by their geometrical areas, scaled by the corresponding angular factors. Simulation results validate our analysis and show the numerical differences between the two models when we vary the frequency and the number of elements in RISs.**

***Index Terms*—Reconfigurable Intelligent Surface (RIS), Intelligent Reflecting Surface (IRS), path-loss model**

I. Introduction

Reconfigurable intelligent surfaces (RISs) have been widely studied in recent years as a promising technology for the next generation of wireless communications, see e.g. [1]. RIS technology has the potential of improving data throughput and energy efficiency by optimizing the environment of wave propagation [2]. By tuning the RIS elements, the RIS can reflect waves toward desired directions to improve network coverage [3].

Recent RIS-related research can be classified as based on the electromagnetic theory and on the communication theory. Understanding and modeling of RIS functionalities of reflection control are the common research focus for both the electromagnetic and communication aspects. Path-loss modeling of signal propagation via RIS reflections is usually one of the main characteristics used in the communication theory analysis. On the other hand, understanding of electromagnetic wave reflections from RIS needs proper electromagnetic-theory studies. Thus, path-loss models form an essential connection between the communication and electromagnetic aspects of RIS studies.

There are several path-loss models for RIS proposed in recent years. For example, the authors in [4] proposed a free-space path-loss model for RIS and validated it via measurement. That model has been implemented and adapted to the Vienna system-level simulator (SLS) for its RIS module. A physics-consistent analytical model in the presence of an RIS is proposed in [5], which is a free-space path-loss model based on the vector generalization of Green's theorem. In [6], the authors used physical optics techniques to derive the path-loss model for an RIS that is configured to reflect an incoming wave from a far-field source towards a receiver in the far-field.

The accuracy of the path-loss model for RIS is crucial for both the communication and electromagnetic studies. However, to the author's best knowledge, there is no deep investigation into these different path-loss models for RIS, and there is no systematic analysis and comparisons of the path-loss models from the communication and electromagnetic point of view. To fill the gap, this paper compares two recently proposed path-loss models for RIS that come from the communication-theory and electromagnetic-theory considerations. We discuss the differences and similarities between them and validate the analysis through simulations.

The remaining part of this paper is organized as follows. Section II introduces the two path-loss models, and Section III provides numerical simulation results from the two models. Conclusions are drawn in Section IV.

II. Introduction of the Path-Loss Models

A. Electromagnetic Model

Recent paper [7] introduced electromagnetic models of links via RIS functioning as an anomalous reflector. In that model, the RIS is modeled as a homogenizable metasurface, whose radiation pattern can be found in terms of the effective electric and magnetic surface currents induced on the metasurface. Under the metasurface framework, the optimized anomalously reflecting RIS carries only one propagating Floquet current harmonic that radiates into the desired direction and a set of evanescent Floquet modes whose field in the far zone can be neglected. The simplest version of the path-loss formula for far-zone links when reflections from supporting walls are negligible, reads

$$P_r = P_t G_t G_r \eta_{\text{eff}} \left(\frac{S_1}{4\pi R_1 R_2} \right)^2 |\cos\theta_i \cos\theta_r|, \qquad (1)$$

where P_r is the received power at the receiving antenna, P_t is the power accepted by the transmitting antenna, G_t and G_r are the gains of the transmitting and the receiving antennas, respectively. Efficiency $\eta_{\text{eff}} < 1$ is a correction parameter for any loss caused by absorption, approximations in design, and imperfections of RIS implementations. S_1 is the geometrical area of the RIS panel. R_1 denotes the distance between the transmitter and the RIS, and R_2 represents the distance between the RIS and the receiver. θ_i and θ_r are the

L. Hao, F. S. Cuesta and S. A. Tretyakov, "Comparison of Simplistic System-Level RIS Models and Diffraction-Theory Solutions," 2024 18th European Conference on Antennas and Propagation (EuCAP), Glasgow, United Kingdom, 2024, pp. 1-5, doi: 10.23919/EuCAP60739.2024.10501069.

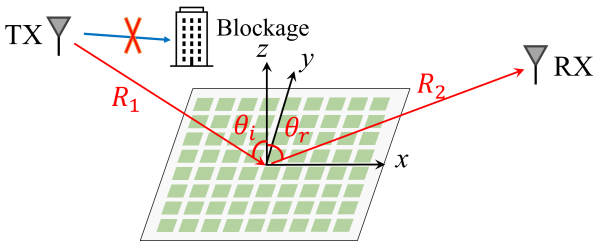

Figure 1: Illustration of the TX-RIS-RX path with the direct path between the BS and the user being blocked.

incidence and reflection angles of signal waves at the RIS position. The angles are counted from the normal to the RIS plane. This model considers an ideal setup, where the RIS is optimized to provide anomalous reflection towards the user at θ_r from the incident waves at θ_i. An illustration of the transmitter-RIS-receiver path is depicted in Fig. 1.

B. Communication Theory Model

A communication theory-based model for RIS-assisted links has been implemented in the Vienna system-level simulator (SLS) [8], [9]. In this model, the received power P_r is calculated as

$$P_r = \frac{P_t G_t G G_r \lambda^2 L A}{64\pi^3 (R_1 R_2)^2}, \tag{2}$$

where G, A, and L are the gain, the effective area of each unit cell, and the total number of unit cells, respectively. The other parameters are the same as in Sec. II-A.

This model assumes a large-scale scenario where there are multiple base stations (BSs), RISs, and users. The BSs and the RISs are not assigned to any user yet, in other words, each user is not aware from which BS and RIS it will receive signals. The model does not account for directivity patterns of the BS, RIS, and the user antennas although they may be included as angular dependencies of the corresponding gains. In this scenario, we define the RIS unit cells in a random configuration, as each RIS does not have any targeted user to serve.

This assumption is made due to the structure of the SLS that first calculates the large-scale fading of each BS-RIS-user link based on the distances between them. Then it performs cell association, to assign BSs to users according to the large-scale fading. Once each BS is assigned to some users, the RIS elements phase can be optimized to serve the associated BS-user pairs. The RIS phase shift optimization is a concept from the communication theory. Basically, it is assumed that the phase shifts of each unit cell are tuned to make them the same as the phase of the BS-user link, so that the users can receive coherent constructive signals from both the direct and RIS-assisted links. This step requires information on the small-scale fadings from the BS-RIS-user and BS-user links, hence, the RIS phase shifts optimization happens in a later step after the small-scale fading of each link is obtained.

After the RIS is optimized to serve the desired user in the desired direction, the received power at the desired user from the BS through the RIS can be calculated in this model as

$$P_r = \frac{P_t G_t G G_r \lambda^2 L^2 A}{64\pi^3 (R_1 R_2)^2}. \tag{3}$$

The difference of factors L^2 in Eq. (3) and L in Eq. (2) comes from the noncoherent combination of electric field for random RIS and coherent combination for optimized RIS, as explained in detail in [9].

In reality, however, RIS elements are strongly coupled, and reflection from RIS is a collective electromagnetic phenomenon that cannot be modeled in terms of effective areas and gains of array elements. It is important to learn to what extent and under what conditions the simplistic communication-theory models can be used.

C. Comparison Between the Two Models

While the communication-theory based Eq. (3) and the electromagnetic model of Eq. (1) have many similarities, there are important differences: note the presence of factor λ^2 and missing angular factors in Eq. (3). Note also that in the electromagnetic model, there is no notion of gain of a single unit cell of a metasurface and that the product LA in Eq. (3) is in general not the same as the RIS area S_1 in Eq. (1). The communication model of Eq. (3) is derived from the assumption that RIS is formed by L small controllable scatterers, neglecting field interactions between the elements. Each element as a small antenna is characterized by its effective area A and gain G. That is, it is assumed that each small antenna receives power equal to the product of the effective area A and the amplitude of the Poynting vector at the antenna location and then re-radiates this power as a transmitting antenna with gain G. However, the received power is defined by the effective area only if the antenna is loaded by the matched load whose resistive part absorbs received power, while the very operational principle of reconfigurable RIS elements is that the antennas are loaded by tunable reactive loads. That is, the antennas are never matched and the received and re-radiated power is never equal to the available power at the antenna port.

As the simplest example, let us assume that RIS is formed by small electric dipole antennas, arranged in a periodical lattice with the period equal to $\lambda/2$. Assuming $\eta_{\text{eff}} = 1$ and substituting $S_1 = L(\lambda/2)^2$ into Eq. (1) we get

$$P_r = \frac{P_t G_t G_r}{(4\pi R_1 R_2)^2} \frac{L^2 \lambda^4}{16} |\cos\theta_i \cos\theta_r|. \tag{4}$$

Let us next substitute the corresponding values of the effective area and gain into (3) and compare the result with the received power calculated with the electromagnetically consistent model of a properly configured RIS of the same size, given by Eq. (4). Gain of a lossless electric dipole antenna equals $G = \frac{3}{2}$, and the effective area can be found using the general relation between the effective area and gain of any reciprocal antenna $A = G\lambda^2/(4\pi)$. Note that the effective area is not equal to the geometrical area of the unit cell that is in our example equal to $\lambda^2/4$. Substitution to Eq. (3) gives

$$P_r = \frac{P_t G_t G_r}{(4\pi R_1 R_2)^2} \frac{9L^2\lambda^4}{64\pi^2}. \quad (5)$$

We see that Eq. (4) and Eq. (5) differ by multiplication factor $\frac{4\pi^2}{9}|\cos\theta_i \cos\theta_r|$. We can try to recover the angular factors assuming that the gain and effective area into the directions of illumination and re-radiation are proportional to the corresponding cosine factors (while in fact the correct factors would be the cosine squared), but the amplitude of the received power is anyway far from the electromagnetic-theory estimate of Eq. (1). Importantly, let us stress again that in this communication-theory model the reflection phase for each antenna element is the same, the one of an antenna tuned to its resonance by loading its port by the complex-conjugate impedance. That is, while the RIS is assumed to be tuned to coherently reflect into the desired direction, the model is for a set of identical dipoles tuned to the resonance. Actually, the effective area and gain are not appropriate parameters for describing response from passive scatterers, the appropriate parameter is the bi-static scattering cross section [10], [11].

On the other hand, if we arbitrarily assume that the effective area of a single element equals the geometrical area of the unit cell ($\lambda^2/4$ in our example) scaled by the angular factor $\cos\theta_r$ and calculate the corresponding gain as $G = 4\pi A/\lambda^2$, scaled by $\cos\theta_i$, we get the same result as the electromagnetic model of Eq. (1)! Indeed, the equation takes the form

$$P_r = \frac{P_t G_t G_r (LA)^2}{(4\pi R_1 R_2)^2} |\cos\theta_i \cos\theta_r|. \quad (6)$$

The factor LA in this equation is the total area of the RIS (if we assume that the unit cells have no gaps between them), which is the same as S_1 in Eq. (1). Now the only difference between Eqs. (6) and (1) is the correction parameter η_{eff}. When we include this parameter in Eq. (6), the two models become the same.

This replacement of the effective area by the geometrical area is wrong from the point of view of the electromagnetic theory (as discussed above, the effective area of a small antenna is not equal to its geometrical area, and the received power of a lossless antenna loaded by a tunable reactance is not defined by the antenna effective area), but it appears that we get the correct estimation for an RIS that is operating as a perfect anomalous reflector.

We stress that this coincidence is valid only for perfectly operating anomalous reflectors where parasitic scattering into all possible reflection directions is completely suppressed. Conventional RIS metasurfaces designed as phase-gradient reflectors always suffer from parasitic scattering [12], meaning that this approach will give some over-estimation of the received power.

Finally we note that the electromagnetic-model formula Eq. (1) can be written in an equivalent form in terms of the effective gain of the RIS panel defined as

$$G_{\text{tx}} = \frac{4\pi S_1}{\lambda^2} |\cos\theta_r| \quad (7)$$

when the RIS is in the transmitting mode and

$$G_{\text{rx}} = \frac{4\pi S_1}{\lambda^2} |\cos\theta_i|, \quad (8)$$

when it is in the receiving mode. Substituting these definitions in Eq. (1) we get

$$P_r = \frac{P_t G_t G_r G_{\text{tx}} G_{\text{rx}} \lambda^4}{(4\pi)^4 (R_1 R_2)^2} \eta_{\text{eff}}. \quad (9)$$

III. Simulation results

In this section, we perform simulations to compare the numerical differences between the two models. We consider an example of a dipole antenna array with $\lambda/2$ spacing between elements. By using the antenna toolbox in MATLAB, we can create a rectangular dipole array with different sizes and tune each element to resonate at a desired frequency. In the simulations, we create a 3×3 rectangular array with resonating dipole antennas as the unit-cell elements, i.e., 9 dipole antennas in this array. We vary the frequency from 20 GHz to 40 GHz. Then for each frequency, we can obtain the radiation pattern of this array and thus also find the total gain of this array. We use the maximum gain of the array to approximate the RIS gains G_{tx} and G_{rx}, respectively. This is reasonable because we can orient the array to make its maximum directivity toward the TX or the RX antennas to imitate the reflection property of an RIS. In addition, we set $\eta_{\text{eff}} = 1$, $G_t = G_r = 1$, and $R_1 = R_2 = 5$ m. The RIS is in the far field of both TX and RX antennas. Then we calculate the path gain as

$$P_{\text{EM}} = \frac{G_t G_r G_{\text{tx}} G_{\text{rx}} \lambda^4}{(4\pi)^4 (R_1 R_2)^2} \eta_{\text{eff}}. \quad (10)$$

from the electromagnetic model (9) and

$$P_{\text{CM}} = \frac{G_t G G_r \lambda^2 L^2 A}{64\pi^3 (R_1 R_2)^2} \quad (11)$$

from the communication model. Note that in Eq. (11) we use $G = \frac{3}{2}$ and $A = \frac{3\lambda^2}{8\pi}$ for each unit cell. The results are shown in Fig. 2, which gives the difference between the two models of around 14.47 dB. This difference comes from the $G_{\text{tx}}G_{\text{rx}}$ in Eq. (10) and $\frac{9L^2}{4}$ with $L = 9$ in Eq. (11) while the remaining terms of the two equations are the same. From the simulation, the maximum gain of the dipole antenna array is almost a constant value of 4.07 dBi over the whole frequency range. It is expected because the gain of a resonant dipole does not depend on the resonance frequency and is a constant value $3/2$.

Since the element number L in Eq. (11) is another important parameter that causes the difference between the two models, we now vary the L value from 3×3, 4×4, ..., 8×8, and create 6 dipole arrays with these 6 different sizes all resonate at 40 GHz. The path gain results from the two models are shown in Fig. 3. The differences between the two models are larger as the number of elements increases. We notice that with the communication model, the path gain increases monotonically with the element number L, which is obvious from Eq. (11). However, with the electromagnetic model, the path gain does not always increase with the element number, because the total gain of an RIS supercell is not proportional to the element number. This is a more general case in reality, otherwise, the antenna gain would be infinitely large when the unit cell number grows to infinity.

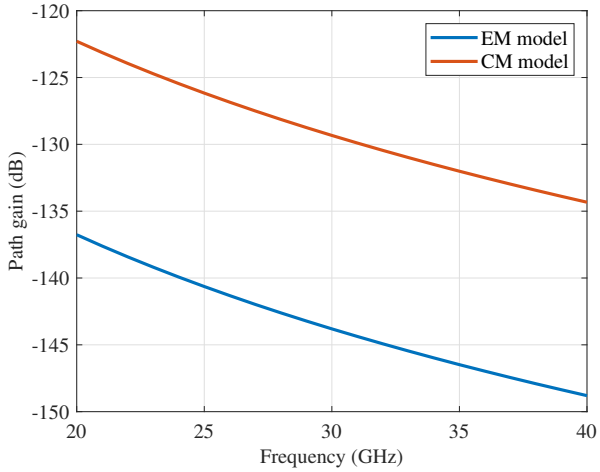

Figure 2: Comparison of the path gain vs. frequency between the electromagnetic (EM) model and communication (CM) model.

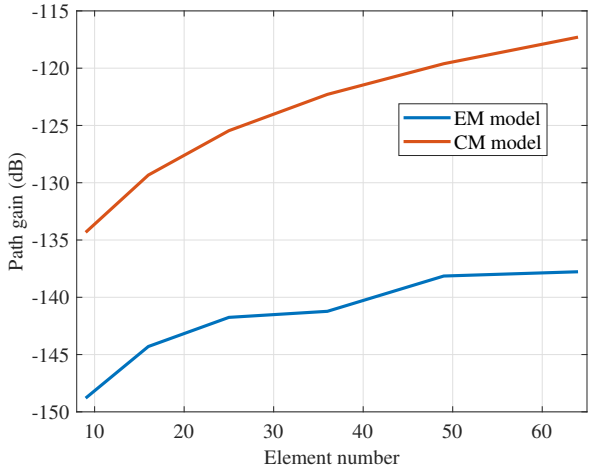

Figure 3: Comparison of the path gain vs. element number between the electromagnetic (EM) model and the communication (CM) model.

On the other hand, the two models become equivalent when the total effective area of the RIS is assumed to be the same for the two models. To simulate such a scenario, We set $LA = S_1|\cos\theta_r|$, $G = 4\pi A|\cos\theta_i|/\lambda^2$, $\theta_i = 50°$, $\theta_r = 0°$, frequency equals to 40 GHz and $A = \lambda^2/4$. Then we vary L from 3 to 40 and compare the results from both Eqs. (3) and (1). The results for both models are shown in Fig. 4, and they are obviously the same. However, we stress that this assumption is in general not valid. To obtain accurate and correct results, the electromagnetic model should be used to model the whole RIS instead of multiplying the element number with the effective area and gain of unit cells. Therefore, the electromagnetic model is implemented as a new path-loss model for RIS-assisted links in the Vienna SLS.

IV. Conclusion

In this contribution, we compared two different path-loss models derived from the electromagnetic and communication theory points of view. The electromagnetic model is derived

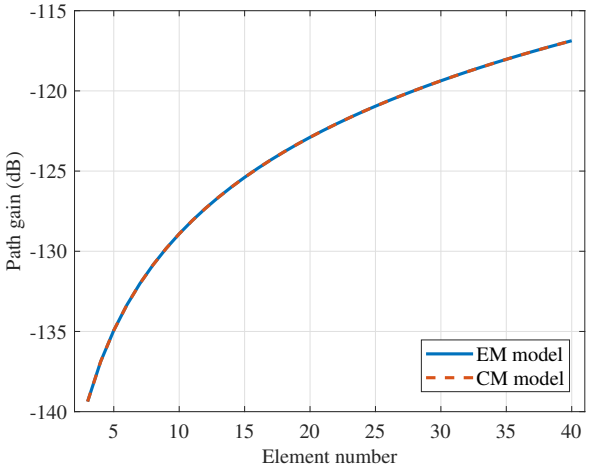

Figure 4: Comparison of the path gain vs. element number between the electromagnetic (EM) model and communication (CM) model in a special case.

modeling the RIS as a metasurface optimized for anomalous reflection into the desired direction. In the communication model, the path-loss model is derived by summing up reflections from all array elements in the assumption that all of them function as independent relays. The properties of each elements are quantified by their effective areas and gains which are not applicable for lossless scatterers. Interestingly, however, if one formally substitutes the effective areas of unit cells by the corresponding geometrical areas scaled by cosine factors, the communication-theory model gives the same result as the electromagnetic one (but only for perfectly functioning RISs). We considered a simple example of a rectangular array with its elements being resonant dipole antennas, in which case the path gain results show about 14.47 dB difference between the two models. The simulation results validate our analysis and demonstrate that in a general case the communication model can give very wrong results. As an improvement, the electromagnetic model has been implemented in the Vienna SLS for RIS-assisted links.

Acknowledgment

This work was partially funded by the European Union's Horizon 2020 research and innovation programme under the Marie Skłodowska-Curie grant agreement No. 956256 and by the Research Council (Academy) of Finland, grant 345178.

References

[1] M. Di Renzo, A. Zappone, M. Debbah, M.-S. Alouini, C. Yuen, J. de Rosny, and S. Tretyakov, "Smart radio environments empowered by reconfigurable intelligent surfaces: How it works, state of research, and the road ahead," *IEEE Journal on Selected Areas in Communications*, vol. 38, pp. 2450–2525, Nov. 2020.

[2] E. Björnson, Ö. Özgecan, and E. G. Larsson, "Intelligent reflecting surface versus decode-and-forward: How large surfaces are needed to beat relaying?," *IEEE Wireless Communications Letters*, vol. 9, p. 244–248, Feb. 2020.

[3] M. A. ElMossallamy, H. Zhang, L. Song, K. G. Seddik, Z. Han, and G. Y. Li, "Reconfigurable intelligent surfaces for wireless communications: Principles, challenges, and opportunities," *IEEE Transactions on Cognitive Communications and Networking*, vol. 6, pp. 990–1002, Sept. 2020.

[4] W. Tang, M. Z. Chen, X. Chen, J. Y. Dai, Y. Han, M. Di Renzo, Y. Zeng, S. Jin, Q. Cheng, and T. J. Cui, "Wireless communications with reconfigurable intelligent surface: Path loss modeling and experimental measurement," *IEEE Transactions on Wireless Communications*, vol. 20, pp. 421–439, Jan. 2021.

[5] F. H. Danufane, M. D. Renzo, J. de Rosny, and S. Tretyakov, "On the path-loss of reconfigurable intelligent surfaces: An approach based on Green's theorem applied to vector fields," *IEEE Transactions on Communications*, vol. 69, pp. 5573–5592, Aug. 2021.

[6] Ö. Özgecan, E. Björnson, and E. G. Larsson, "Intelligent reflecting surfaces: Physics, propagation, and pathloss modeling," *IEEE Wireless Communications Letters*, vol. 9, pp. 581–585, May 2020.

[7] S. Kosulnikov, F. S. Cuesta, X. Wang, and S. A. Tretyakov, "Simple link-budget estimation formulas for channels including anomalous reflectors," *IEEE Transactions on Antennas and Propagation*, vol. 71, pp. 5276–5288, June 2023.

[8] L. Hao, A. Fastenbauer, S. Schwarz, and M. Rupp, "Towards system level simulation of reconfigurable intelligent surfaces," in *2022 International Symposium ELMAR*, pp. 81–84, Sept. 2022.

[9] L. Hao, S. Schwarz, and M. Rupp, "The extended Vienna system-level simulator for reconfigurable intelligent surfaces," in *2023 Joint European Conference on Networks and Communications & 6G Summit (EuCNC/6G Summit)*, pp. 1–6, July 2023.

[10] F. T. Ulaby, *Fundamentals of Applied Electromagnetics*. Upper Saddle River, N.J.: Prentice Hall, 5th edition ed., 2007.

[11] C. A. Balanis, *Antenna Theory Analysis and Design*. Hoboken: Wiley, 3rd ed., 2005.

[12] A. Díaz-Rubio, V. S. Asadchy, A. Elsakka, and S. A. Tretyakov, "From the generalized reflection law to the realization of perfect anomalous reflectors," *Sci. Adv.*, vol. 3, p. e1602714, Aug. 2017.